

Supplemental Material

Synthetic Approaches to (smif)₂Ti (smif = 1,3-di-(2-pyridyl)-2-azaallyl) Reveal Redox Non-Innocence and C-C Bond-Formation

Brenda A. Frazier,^a Peter T. Wolczanski*,^a Ivan Keresztes,^a Serena DeBeer,^a Emil B. Lobkovsky,^a Aaron W. Pierpont,^b and Thomas R. Cundari^b

^aDepartment of Chemistry & Chemical Biology, Baker Laboratory, Cornell University, Ithaca, New York 14853 (USA); E-mail: ptw2@cornell.edu

^bDepartment of Chemistry, Center for Advanced Scientific Computing and Modeling (CASCaM), University of North Texas, Box 305070, Denton, Texas 76203-5070

	page
I. NMR Spectroscopic Structure Elucidation	S2
II. Product Ratios from Synthetic Attempts toward "(smif)₂Ti".	S12
III. ¹H NMR Spectrum Obtained from Trial 14 Toward Synthesis of (smif){Li(smif-smif)}Ti (1)	S 13

I. **NMR Spectroscopic Structure Elucidation.** With the crystal structure of (smif){Li(smif-smif)}Ti (**1**) determined, NMR spectroscopy was used to investigate **1** in solution to see if its solid state conformation was retained. During spectral acquisition, **1** degraded to give substantial quantities of [(smif)Ti]₂(μ-κ³,κ³-N,N(py)₂-smif,smif) (**2**) within 30 min, and further decomposition to (smif)Ti(κ³-N,N(py)₂-smif,(smif)H) (**3**) and (smif)Ti(dmpa) (**4**) occurred over extended periods. A rough mixture of **1-4** was conveniently obtained for spectroscopic purposes upon heating **1** at 80°C for 44 h, and compound **4** was observed to be the last to form. A ¹H NMR spectrum containing 76 inequivalent protons

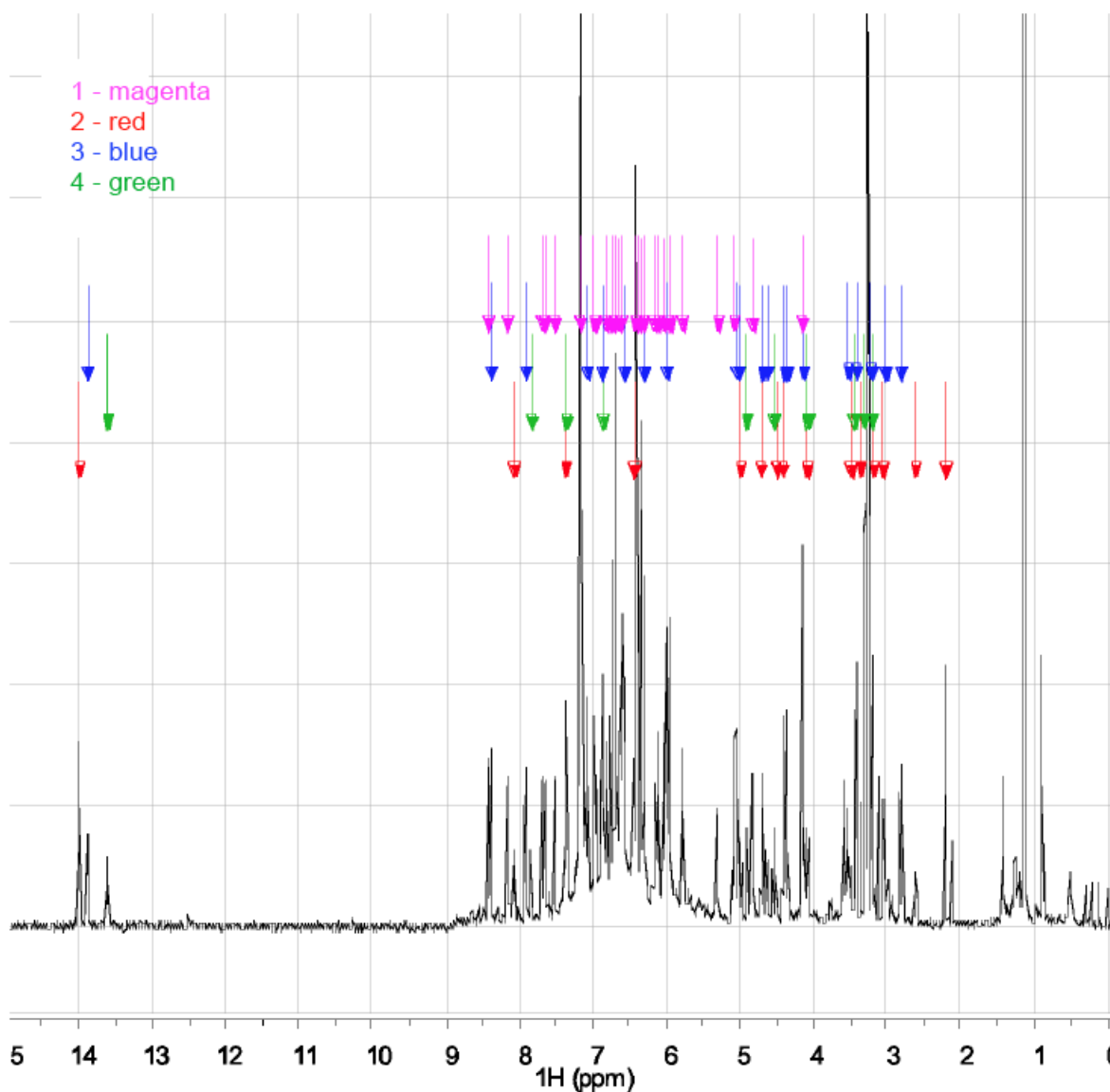


Figure S1. ¹H NMR spectrum of (smif){Li(smif-smif)}Ti (**1**, magenta), [(smif²⁻)Ti^{III}]₂(μ-κ³,κ³-N,N(py)₂-smif,smif) (**2**, red), (smif)Ti(κ³-N,N(py)₂-smif,(smif)H) (**3**, blue), and (smif)Ti(dmpa) (**4**, green) in C₆D₆.

(Fig. S1). Three pyridine *ortho*-CH peaks appeared, shifted significantly downfield from the rest of the rings, and were indicative of three different titanium compounds (δ 13.88, [(smif²⁻)Ti^{III}]₂(μ - κ^3 , κ^3 -N,N(py)₂-smif,smif) (**2**); δ 13.99, (smif)Ti(κ^3 -N,N(py)₂-smif,(smif)H) (**3**); δ 13.61, (smif)Ti(dmpa) (**4**). Monitoring the mixture during thermolysis (80 °C for over 16 d) enabled the identification of ¹H chemical shifts corresponding to **4**, as it was the last species to grow in. In order to elucidate the identity of the four compounds in solution, a series of two-dimensional (2-D) NMR spectroscopic experiments were employed.

Initial efforts to identify the species in solution focused on utilizing 2-D correlation spectroscopy (COSY), which facilitated the identification of protons that were spin coupled to one another, specifically adjacent protons on the pyridine rings. From these correlations, the gCOSY spectrum elucidated the possibility of 15 different pyridine rings, and the proton with the most downfield chemical shift

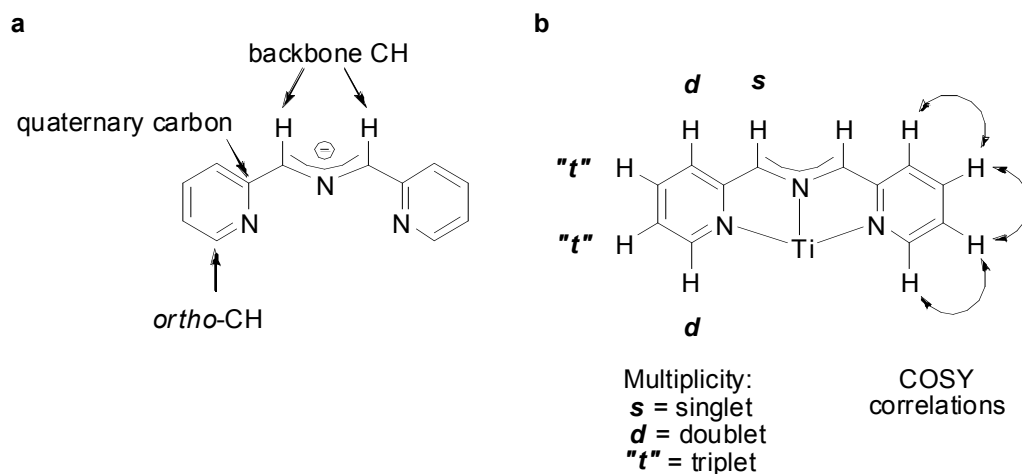


Figure S2. **a.** Pyridine ring and ligand nomenclature. **b.** ¹H NMR splitting pattern (left ring) and COSY correlations typically observed denoted with arrows (right ring).

corresponded to the pyridine *ortho*-CH in most cases (Fig. S2). Four pyridine rings (*ortho*-CH δ 13.99, 13.88, 7.65, 7.17 ppm) were completely assembled as a result of distinct proton chemical shifts and strong COSY correlations exhibited within the typical aromatic region. Strong cross peaks existed for at least five other pyridine rings (*ortho*-CH δ 8.42, 8.38, 8.15, 7.65, 7.51 ppm); however, overlapping signals observed around 6.30, 6.40, and 6.73 ppm hindered the precise assignment of ¹H chemical shifts. In

contrast to the strong correlations observed for the aforementioned rings, all pyridine rings shifted upfield from the aromatic region displayed weaker COSY correlations. One of these pyridines, which was shifted significantly upfield (*ortho*-CH δ 4.12 ppm), was established through the weak COSY correlations observed between all four protons within the ring system. A unique set of cross peaks indicated that two triplets (δ 4.63, 3.52 ppm) were coupled to the same "doublet" (δ 5.03 ppm), whose chemical shift was consistent with a pyridine *ortho*-CH relative to the triplets, thus ambiguity complicated the ring assignment. Correlations between all proton sets within a ring were not observed for at least five other possible rings. In addition to identifying pyridine rings, the COSY spectrum displayed a cross peak consistent with the interior CHs (δ 4.82, 5.30 ppm) on the coupled ligand in (smif){Li(smif-smif)}Ti (**1**). Unfortunately, due to overlapping cross peaks and weak correlations, all 15 rings were not solely assembled through gCOSY.

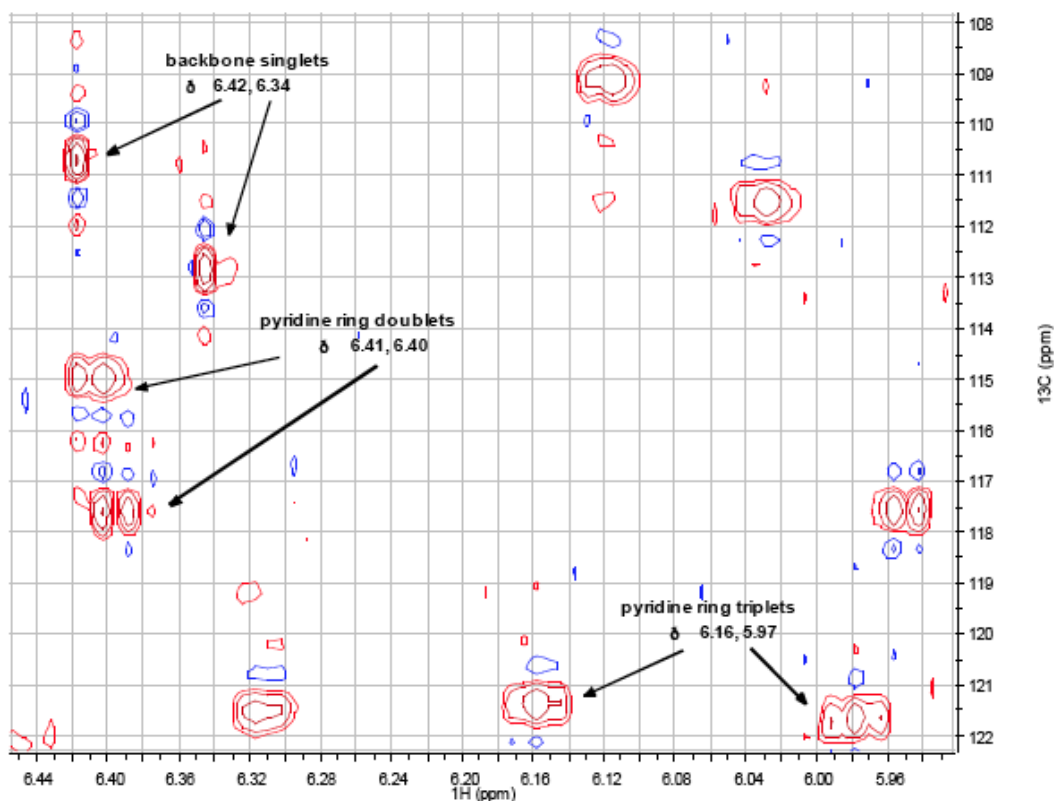


Figure S3. Examples of multiplicities observed in HSQCAD of (smif){Li(smif-smif)}Ti (**1**), [(smif²⁻)Ti^{III}]₂(μ - κ^3 , κ^3 -N,N(py)₂-smif,smif) (**2**), (smif)Ti(κ^3 -N,N(py)₂-smif,(smif)H) (**3**), and (smif)Ti(dmpa) (**4**) in C₆D₆.

Adiabatic heteronuclear single quantum coherence (HSQCAD) 2-D spectroscopy displayed correlations between 75 protons and their adjacent carbons. Each correlation portrayed the multiplicity of the proton (Figure S3). Consequently, backbone CHs and pyridine ring protons were easily recognized. The diverse ^{13}C chemical shifts aided in differentiating between ^1H chemical shifts (δ 6.74, 6.73, 6.41, 6.40, 6.31, 6.30, 5.04, 5.02 ppm) in areas containing a cluster of overlapping ^1H NMR signals and COSY correlations, thus helping to elucidate six pyridine rings. Additionally, HSQCAD revealed new ^1H - ^{13}C correlations, which went undetected in the COSY presumably due to weak correlations. This accounted for eight pyridine ring signals as well as fifteen backbone CH signals, thereby indicating a total of fifteen pyridine rings. Ultimately, the presence of an NH peak, observed in $(\text{smif})\text{Ti}(\kappa^3\text{-N,N}(\text{py})_2\text{-smif},(\text{smif})\text{H})$ (**3**), was established through a lacking HSQCAD cross peak for the remaining proton (δ 3.01 ppm).

The quaternary carbons of all 15 pyridine rings were identified through the strong correlation observed with the pyridine ring's *ortho*-CH via the 2-D NMR experiment gHMBCAD (adiabatic heteronuclear multiple bond correlation). This spectroscopy also gave rise to a variety of other cross peaks useful for arranging protons around the pyridine rings as each ring portrayed the same correlation patterns and ^{13}C chemical shifts within a ring also portrayed a distinct pattern (Figure S4). Ligand fragments were established by correlations observed between pyridine rings and their adjacent backbone CH/CH₂ groups. These fragments were assembled to form eight different ligand environments via the cross peaks observed between a backbone proton and a carbon from the other fragment. Four symmetric

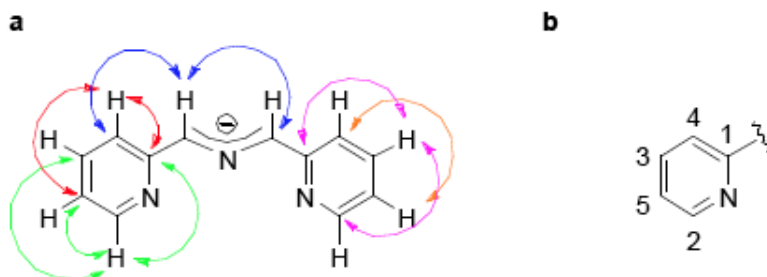


Figure S4. a. Typical correlations observed in gHMBCAD. b. Ordering of ^{13}C chemical shifts within a pyridine ring (highest shift 1, lowest shift 5).

and four asymmetric smif ligand environments were established. The spectroscopy verified $[(\text{smif}^2)\text{Ti}^{\text{III}}]_2(\mu\text{-}\kappa^3, \kappa^3\text{-N,N}(\text{py})_2\text{-smif,smif})$ (**2**) contained one symmetric ligand via the self-correlation (δ 2.19 (^1H) with 74.93 (^{13}C) ppm). In the case of $(\text{smif})\text{Ti}(\text{dmpa})$ (**4**), the gHMBCAD correlations (δ 3.43 (^1H) with 108.43 (^{13}C), 3.29 (^1H) with 61.83 (^{13}C) ppm) were indicative of two symmetric ligand environments. $(\text{smif})\text{Ti}(\kappa^3\text{-N,N}(\text{py})_2\text{-smif,}(\text{smif})\text{H})$ (**3**) also contained a symmetric ligand (δ 4.38 (^1H) with 73.85 (^{13}C) ppm). The gHMBCAD experiment aided in verifying pyridine ring assignments established through gCOSY.

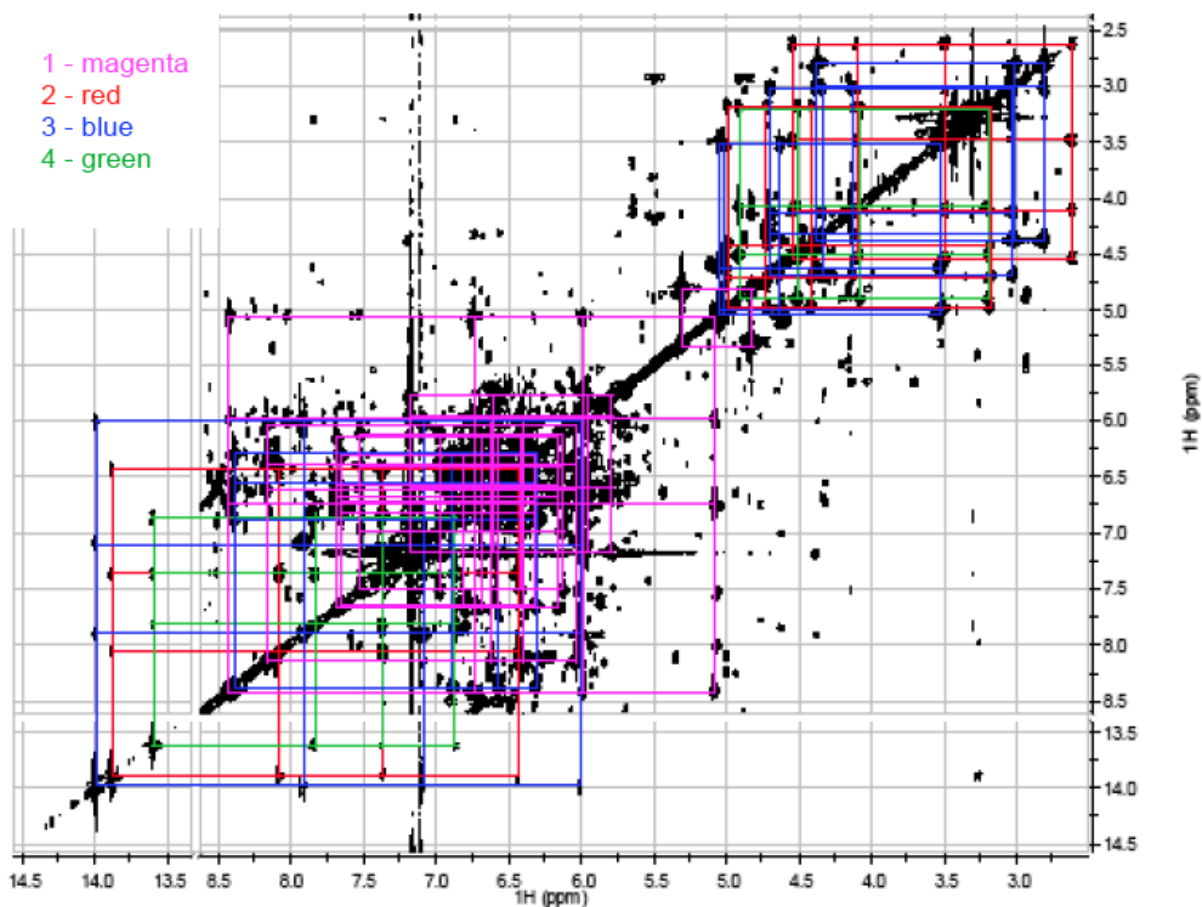


Figure S5. Complete TOCSY obtained for $(\text{smif})\{\text{Li}(\text{smif-smif})\}\text{Ti}$ (**1**, magenta), $[(\text{smif}^2)\text{Ti}^{\text{III}}]_2(\mu\text{-}\kappa^3, \kappa^3\text{-N,N}(\text{py})_2\text{-smif,smif})$ (**2**, red), $(\text{smif})\text{Ti}(\kappa^3\text{-N,N}(\text{py})_2\text{-smif,}(\text{smif})\text{H})$ (**3**, blue), and $(\text{smif})\text{Ti}(\text{dmpa})$ (**4**, green) in C_6D_6 .

In order to finish assigning the 15 pyridine rings, total correlation spectroscopy (TOCSY) was utilized since all protons within a specific spin system produced a series of cross peaks. The overall TOCSY spectrum appeared quite overwhelming initially (Figure S5). Each pyridine ring contained its own spin system, and all protons corresponding to one ring appeared in a line, subsequently verifying assignments made based upon other 2-D spectra (see Figures S6-S9). Additionally, this experiment was particularly useful in differentiating pyridine rings that were hard to discern from the gCOSY and gHMBCAD due to overlapping cross peaks. The TOCSY spectrum for (smif)Ti(κ^3 -N,N(py)₂-smif,(smif)H) (**3**), shown in Figure S9, corroborated the presence of five ring systems. Four rings were previously confirmed as pyridine rings, and the remaining ring corresponded to the substituted piperazine generated via ligand coupling. Interestingly, the TOCSY spectrum consistently displayed peaks connecting the backbone CH to the pyridine rings containing upfield chemical shifts.

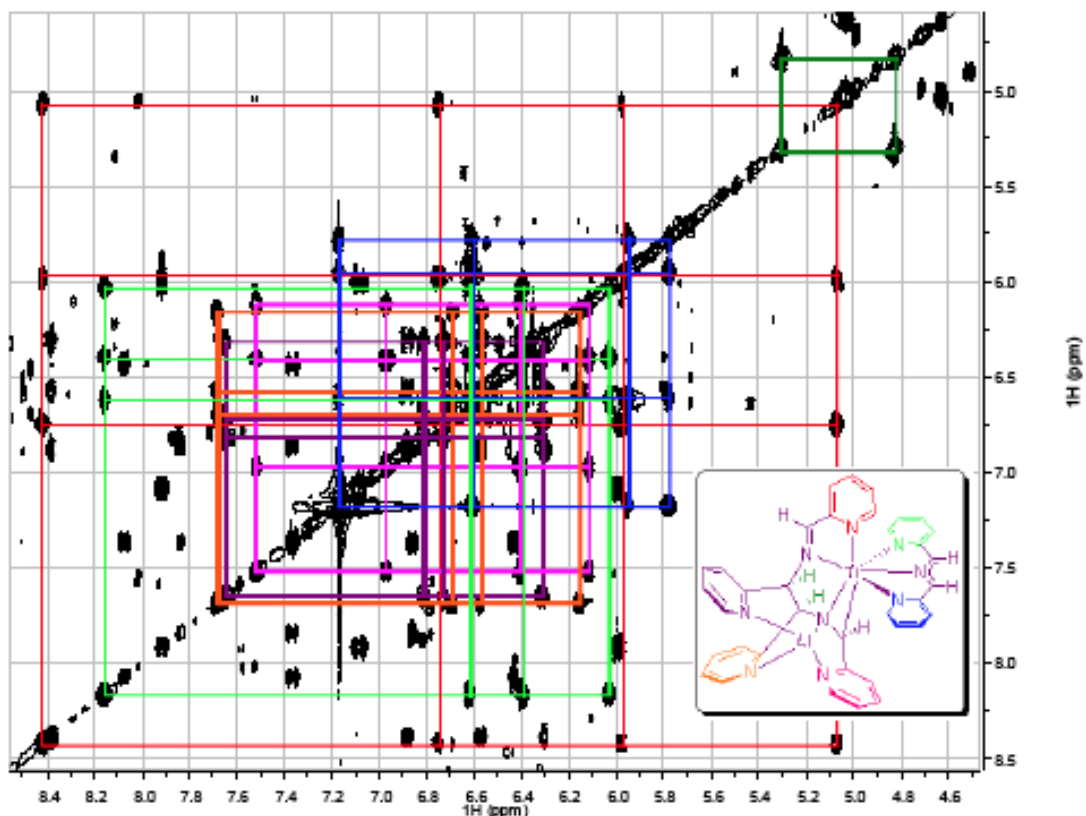


Figure S6. TOCSY depicting correlations for (smif){Li(smif-smif)}Ti (**1**).

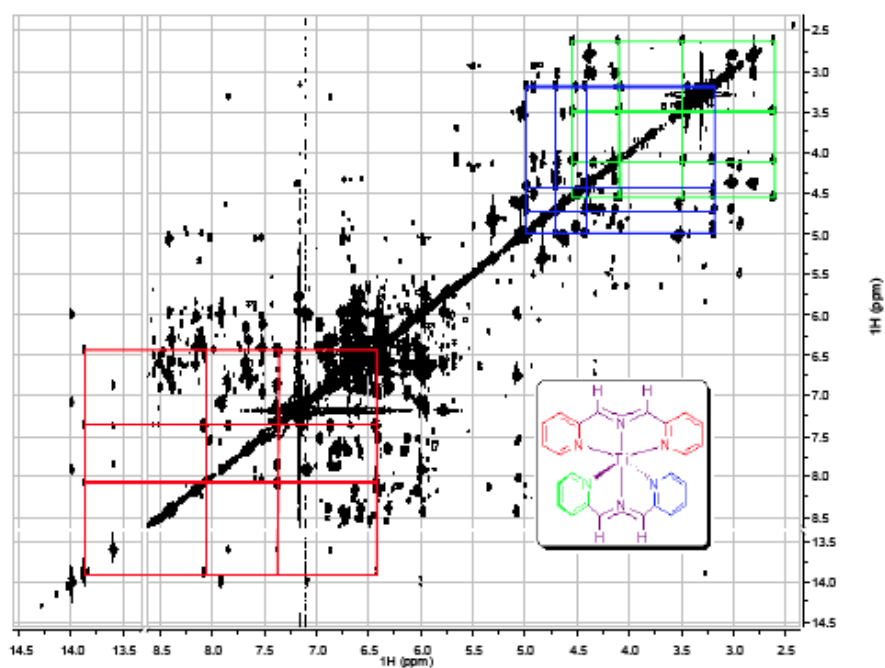


Figure S7. TOCSY highlighting correlations for $[(\text{smif}^2)\text{Ti}^{\text{III}}]_2(\mu\text{-}\kappa^3, \kappa^3\text{-N,N}(\text{py})_2\text{-smif,smif})$ (**2**).

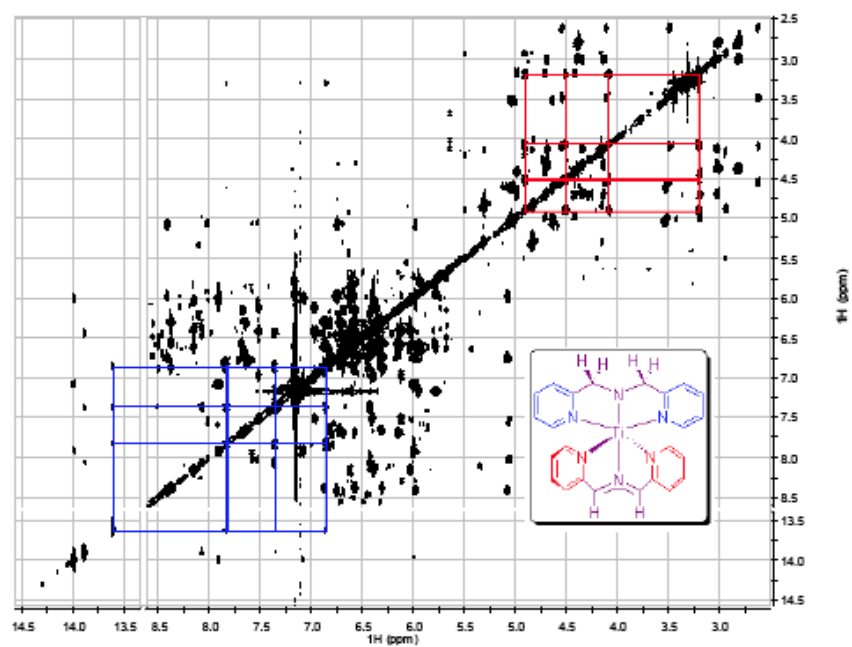


Figure S8. TOCSY showing correlations for $(\text{smif})\text{Ti}(\text{dmpa})$ (**4**).

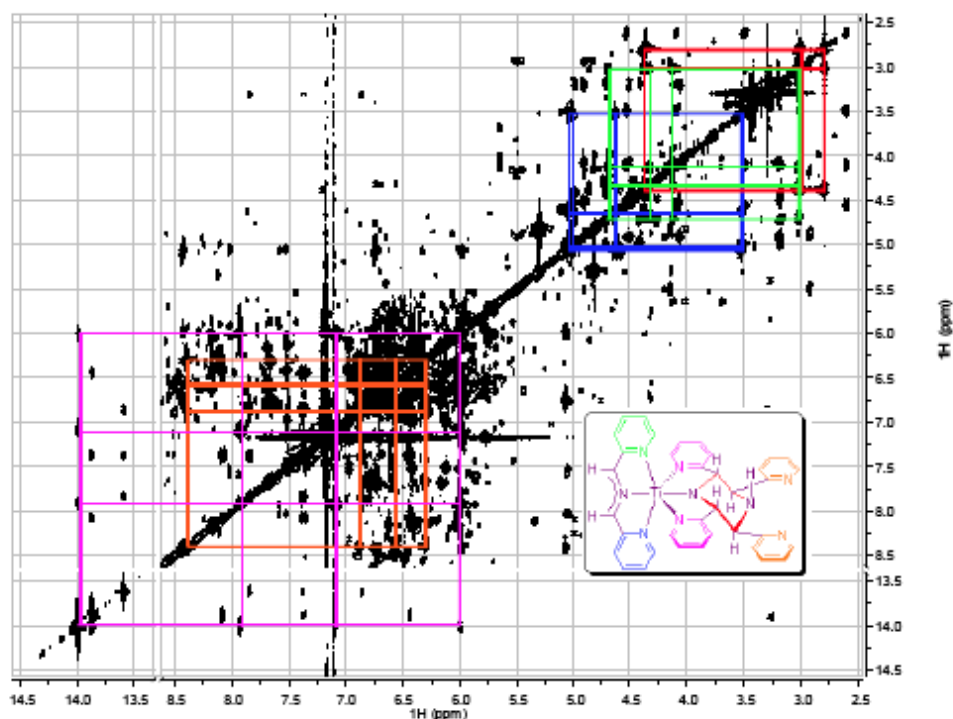


Figure S9. TOCSY emphasizing correlations for $(\text{smif})\text{Ti}(\kappa^3\text{-N,N}(\text{py})_2\text{-smif},(\text{smif})\text{H})$ (**3**).

Rotating-frame overhauser effect spectroscopy (ROESY) determined which ligand environments were associated with a specific titanium center. Furthermore, ROESY revealed the spatial orientation of the ligands surrounding titanium. In the case of $(\text{smif})\{\text{Li}(\text{smif-smif})\}\text{Ti}$ (**1**), ROESY cross peaks were seen for the four protons of coupled ligand's backbone (δ 4.15, 4.82, 5.30, 6.70 ppm) indicating they were all on the same side of the molecule. Strong correlations were observed between two of the aforementioned backbone CHs (δ 4.82, 5.30 ppm) and the pyridine *ortho*-CH (δ 8.15 ppm) on the smif ligand indicating the direction in which the smif ligand should lie. Weak correlations existed between the remaining backbone CHs (δ 4.15, 6.70 ppm) and the smif ligand's pyridine *ortho*-CH (δ 8.15 ppm). The other pyridine *ortho*-CH on the smif ligand (δ 7.17 ppm) only showed a correlation with the adjacent pyridine ring proton (δ 5.78 ppm). The smif ligand backbone CHs (δ 6.34, 6.42 ppm) exhibited cross peaks with the pyridine *ortho*-CH at δ 8.42 ppm. For $[(\text{smif}^2)\text{Ti}^{\text{III}}]_2(\mu\text{-}\kappa^3,\kappa^3\text{-N,N}(\text{py})_2\text{-smif,smif})$ (**2**), the symmetric smif ligand backbone (δ 2.19 ppm) and the pyridine *ortho*-CHs (δ 3.49, 4.71 ppm) on the asymmetric smif

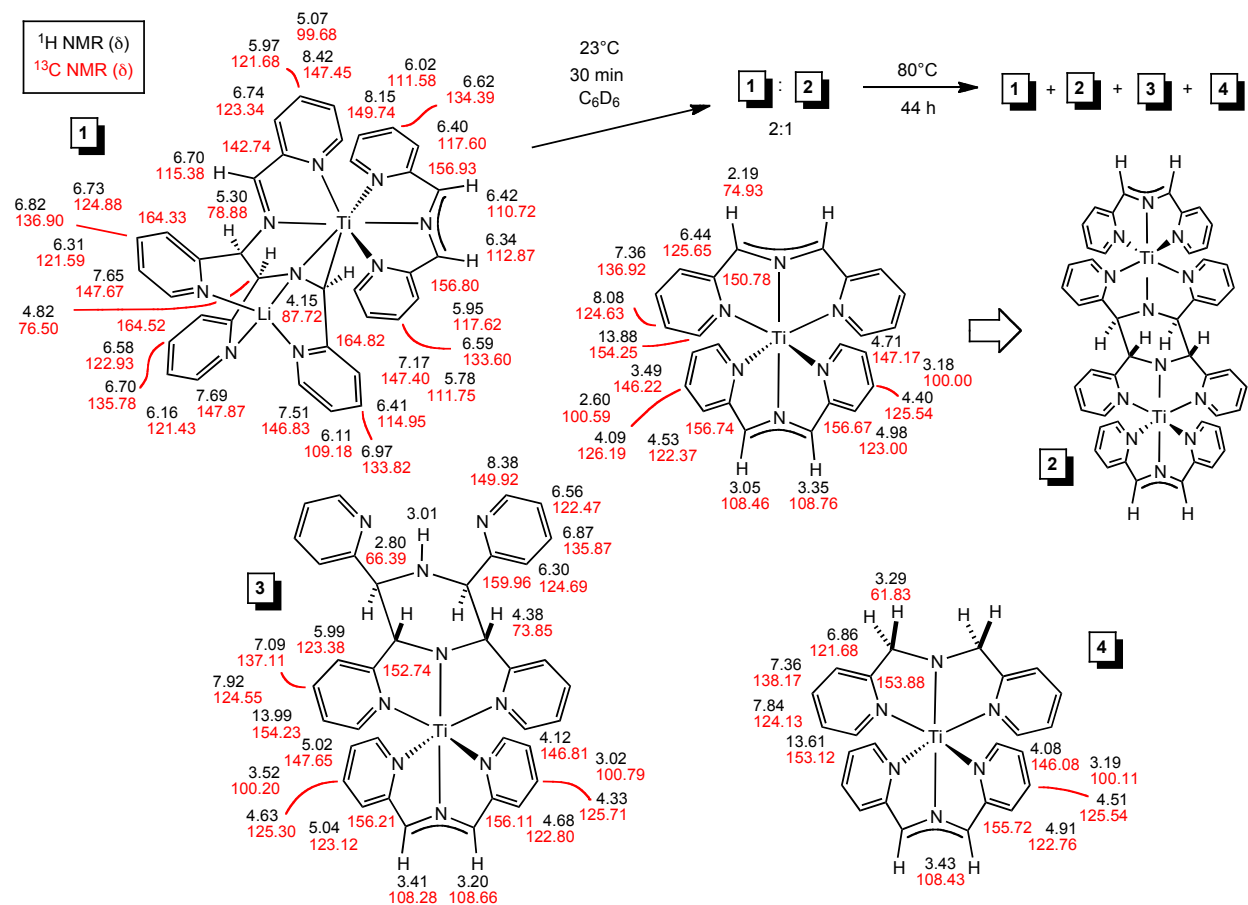


Figure S10. NMR spectral assignments of (smif)₂{Li(smif-smif)}Ti (**1**), [(smif²⁻)Ti^{III}]₂(μ-κ³,κ³-N,N(py)₂-smif,smif) (**2**), (smif)Ti(κ³-N,N(py)₂-smif,(smif)H) (**3**), and (smif)Ti(dmpa) (**4**) in C₆D₆.

ligand gave rise to cross peaks. No correlation was seen between the symmetric ligand's pyridine *ortho*-CH (δ 13.88 ppm) and the backbone CHs (δ 3.05, 3.35 ppm) for the asymmetric smif. The ROESY for (smif)Ti(dmpa) (**4**) revealed that the two ligand environments were situated perpendicular to one another. The smif backbone CH (δ 3.43 ppm) and the di(2-pyridylmethyl)amine (dpma) pyridine *ortho*-CH (δ 13.61 ppm) displayed a weak correlation while the backbone CH₂ groups (δ 3.29 ppm) on dpma and the pyridine *ortho*-CH (δ 4.08 ppm) on smif exhibited a strong correlation. For (smif)Ti(κ³-N,N(py)₂-smif,(smif)H) (**3**), the orientation of the asymmetric smif ligand with respect to the coupled ligand was based on the ROESYs observed between the pyridine *ortho*-CH and the coupled ligand's backbone CHs. One pyridine *ortho*-CH (δ 5.02 ppm) correlated solely to a single backbone CH (δ 2.80 ppm), while the

other *ortho*-CH (δ 4.12 ppm) gave rise to a cross peak with both the backbone CH (δ 4.38 ppm) and NH (δ 3.01 ppm). The asymmetric smif backbone CHs (δ 3.20, 3.41 ppm) both displayed correlations with the pyridine *ortho*-CH (δ 13.99 ppm) on the coupled ligand, indicative of a mirror plane within the ligand framework. Complete NMR spectroscopic assignments for compounds **1-4** can be found in Scheme 2 in the paper and Figure S10 above, and coupling constant information is given in the Experimental.

II. Product Ratios from Synthetic Attempts toward "(smif)₂Ti".

Table S1. Product Ratios from Synthetic Attempts toward "(smif)₂Ti".

Trial	Ti source	smif source	solvent	Red Agt	T(°C)	time	1	2	3	4
1	TiCl ₃ (THF) ₃	Li(smif)	DME	1 Na/Hg	0-23	16 h	3	1	0	0.75
2	TiCl ₃ (THF) ₃	Li(smif)	DME	1 Na/Hg	0-23	16 h	1	1	0	0
3	TiCl ₃ (THF) ₃	Li(smif)	DME	1 Na/Hg	0-23	16 h	1	0.5	0	0.5
4 ^a	TiCl ₃ (THF) ₃	Li(smif)	DME	1 Na/Hg	0-23	16 h	2	1	0	1
5 ^b	TiCl ₃ (THF) ₃	Li(smif)	DME	1 Na/Hg	0-23	2 d	0	1	1	0
6 ^c	TiCl ₃ (THF) ₃	Li(smif)	THF	1 Na/Hg	-78-23	14 h	0	1	0.25	2
7 ^c	TiCl ₃ (THF) ₃	Li(smif)	THF	1 Na/Hg	-78-23	16 h	0	1	0.7	0
8	TiCl ₃ (THF) ₃	Li(smif)	THF	1 Na/Hg	-78-23	16 h	0	1	0.25	0.75
9	TiCl ₃ (THF) ₃	Li(smif)	THF	1 Na/Hg	-78-23	16 h	0	1	0	0
10	TiCl ₃ (THF) ₃	Li(smif)	THF	1 Na/Hg	-78-23	16 h	2	1	0	0
11	TiCl ₃ (THF) ₃	Li(smif)	THF	1 Na/Hg	-78-23	16 h	0	1	0	0
12 ^d	TiCl ₃ (THF) ₃	Li(smif)	THF	1 Na/Hg	-78-23	16 h	0	1	0	0
13 ^e	TiCl ₃ (THF) ₃	Li(smif)	THF	1 Na/Hg	-78-23	2.5 d	0	1	0	1
14	TiCl ₃ (THF) ₃	Li(smif)	THF	2 Na/Hg	-78-23	12 h	4	1	0	0.5
15	TiCl ₃ (THF) ₃	Li(smif)	THF	Li(smif)	-78-23	36 h	0	0	1	0
16 ^f	TiCl ₃ (THF) ₃	Li(smif)	THF	0.5 Mg	-78-23	12 h	0	0.5	0	0.5
17	TiCl ₃	Li(smif)	DME	1 Na/Hg	0-23	18 h	0	1	0	0.5
18	TiCl ₃	Li(smif)	DME	1 Na/Hg	0-23	18 h	0	1	0	1
19	TiCl ₃	Li(smif)	DME	2 Na/Hg	0-23	18 h	0	1	0	0.25
20	CITi{N(TMS) ₂ THF	H(smif)	THF	1 Na/Hg	-78-23	16 h	0	0	0	0
21 ^g	TiCl ₄ (THF) ₂	Li(smif)	THF	2 Mg	-78-23	16 h	0	0	0	0
22	TiCl ₄ (THF) ₂	Li(smif)	THF	2 Na/Hg	-78-23	8 h	0	1	0	0
23	TiCl ₄ (THF) ₂	Li(smif)	THF	2 Na/Hg	-78-23	16 h	0	1	1	0
24	TiCl ₄ (THF) ₂	Li(smif)	THF	2 Na/Hg	-78-23	16 h	0	3	1	0
25	TiCl ₂ (TMEDA) ₂	Na(smif)	C ₆ D ₆		23	17.5 h	0	1	0	3
26	TiCl ₂ (TMEDA) ₂	Na(smif)	C ₆ D ₆		23	21.5 h	0	0.18	0	3
27	TiCl ₂ (TMEDA) ₂	Na(smif)	C ₆ D ₆		23	2.5 d	0	0	0	1
28	TiCl ₂ (TMEDA) ₂	(smif) ₂ Mg (5)	C ₆ D ₆		23	15 h	0	0	0	0
29	TiCl ₂ (TMEDA) ₂	(smif) ₂ Zn	C ₆ D ₆		23	17.5 h	0	1	0	1
30	TiCl ₂ (TMEDA) ₂	Na(smif)	THF- <i>d</i> ₈		23	21.5 h	0	0.25	0	1
31	TiCl ₂ (TMEDA) ₂	Na(smif)	THF- <i>d</i> ₈		23	3.75 d	0	2.5	6.5	0
32	TiCl ₂ (TMEDA) ₂	Na(smif)	THF		-78-23	18 h	0	1	0	0
33	TiCl ₂ (TMEDA) ₂	(smif) ₂ Mg (5)	THF		-78-23	2 d	0	0	0	0
34	TiCl ₂ (TMEDA) ₂	(smif) ₂ Zn	THF		-78-23	2 d	0	0	0	0

^aAlso 27 equiv Li(smif). ^bAlso 11 equiv Li(smif). ^cOther unidentified species present. ^dSilated glassware. ^eAlso 32 equiv Li(smif). ^fAlso, 1 equiv (smif)₂Mg (**5**) and 9 equiv (smif)MgCl. ^gOnly (smif)MgCl present.

III. ^1H NMR Spectrum Obtained from Trial 14 Toward Synthesis of $(\text{smif})\{\text{Li}(\text{smif-smif})\}\text{Ti}$ (1)

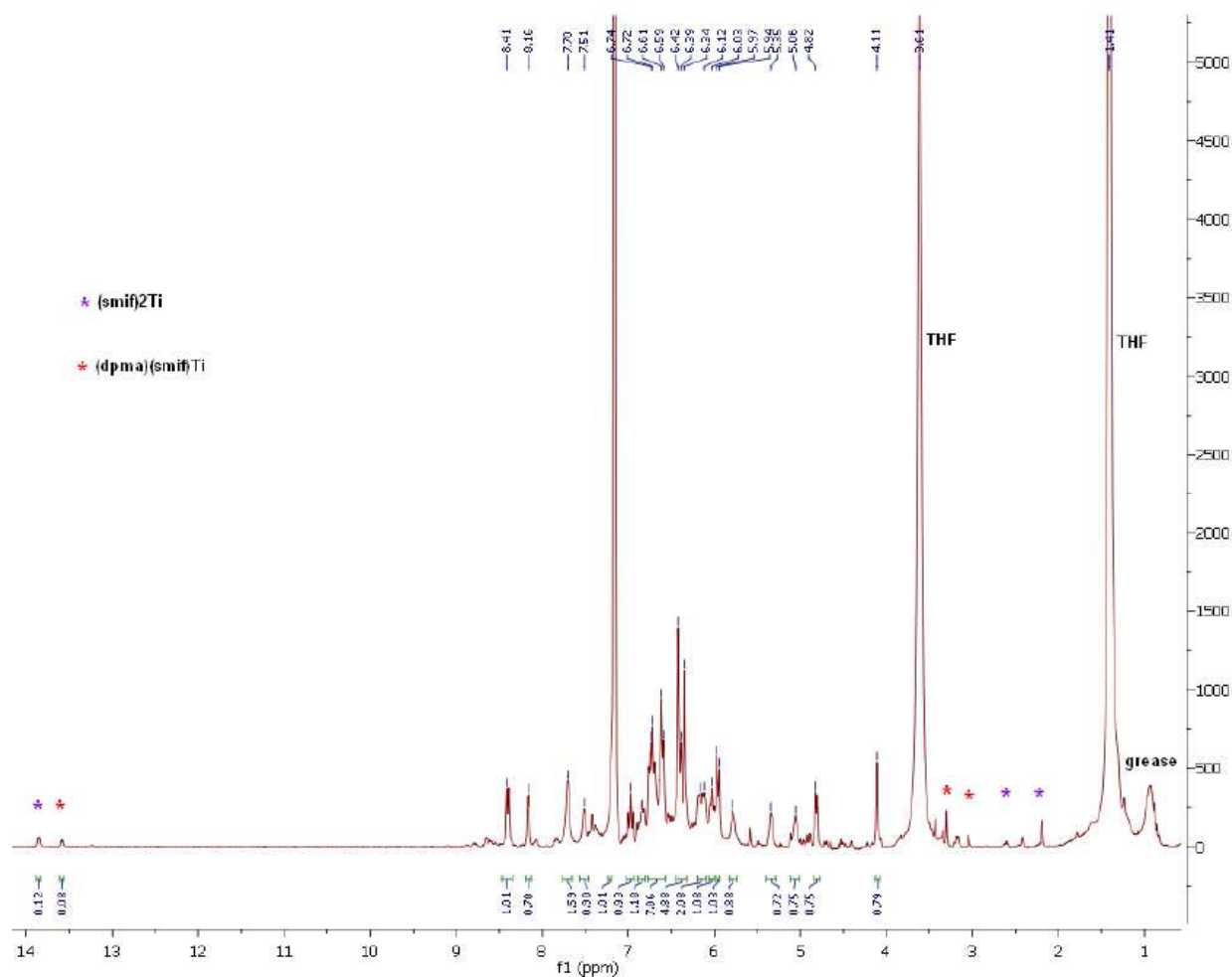


Figure S10. Dissolution of X-ray quality crystal of $(\text{smif})\{\text{Li}(\text{smif-smif})\}\text{Ti}$ (**1**) obtained via trial 14, and as given in experimental procedure **3**. ^1H NMR spectrum (C_6D_6) reveals residual THF, ~80% **1** and ~20% formation of $[(\text{smif}^2)\text{Ti}^{\text{III}}]_2(\mu\text{-}\kappa^3, \kappa^3\text{-N,N}(\text{py})_2\text{-smif,smif})$ (**2**, signals indicated by *) within the 10 min it took to obtain the spectrum.